Geomechanics and Engineering, *Vol. 27, No. 2 (2021) 189-196*
https://doi.org/10.12989/gae.2021.27.2.189

Seismic stability analysis for a two-stage slope

Pingping Rao*[1], Jian Wu[1a], Ganyou Jiang[2b], Yunwei Shi[3c], Qingsheng Chen[4d] and Sanjay Nimbalkar[5e]

[1]*Department of Civil Engineering, University of Shanghai for Science and Technology, Shanghai 20093, China*
[2]*Guangxi Luqiao Engineering Group Co., Ltd., Nanning 530011, China*
[3]*School of Naval Architecture, Ocean and Civil Engineering, Shanghai Jiaotong University, Shanghai 200240, China*
[4]*Hubei Provincial Ecological Road Engineering Technology Research Center, Hubei University of Technology, Wuhan, 430068, China*
[5]*School of Civil and Environmental Engineering, University of Technology Sydney, 15 Broadway Ultimo NSW 2007, Australia*

(Received April 1, 2019, Revised March 24, 2021, Accepted October 7, 2021)

Abstract. This paper adopts the kinematic theorem of limit analysis to assess the seismic stability of a two-stage slope. The seismic effect is taken into account by using the pseudo-static approach. The failure mechanism for the slope is extended to include below-toe failure, toe failure and face failure. Validation of this approach is conducted by comparing the factor of safety with the data in the existing literatures. The stability charts are presented based on the graphical method for reading the factor of safety readily. Parametric study involving the effect of slope geometry, internal friction angle, seismic effect as well as depth coefficient on the stability of a two-stage slope is carried out. The critical failure surfaces with various parameters are plotted. The results obtained reveal the significant influence of slope geometry on the failure mechanism of a two-stage slope under static and seismic condition.

Keywords: critical failure surface; limit analysis; safety factor; seismic stability; two-stage slope

1. Introduction

Landslide is one of the worst natural disasters. The worldwide earthquake-induced landslides over the years have resulted in serious casualties and damages to properties, therefore the assessment of the slope stability remains a long-standing topic in geotechnical engineering. Approaches to assess the stability of slopes can be mainly categorized into three groups: (1) limit equilibrium method, (2) numerical approaches and (3) limit analysis method. The most common method used for slope stability analysis over the past decades is the limit equilibrium method (Lam and Fredlund, 1993, Shukla *et al.* 2009, Deng *et al.* 2017, Motlagh *et al.* 2018). However, due to the assumptions related to the internal force distribution, the solution obtained is neither an upper bound nor a lower bound of the true solution. Numerical approaches such as finite-element method and finite-difference method are also used for slope stability assessment (Cai and Ugai 2000, Shen and Abbas 2013, Aksoy *et al.* 2016, Kim and Jeong 2017, Yang *et al.* 2017, Babanouri and Sarfarazi 2018, Tran *et al.* 2019). But the high computational cost and intensive invested efforts make the numerical approaches less attractive. In contrast, the kinematic theorem of limit analysis can find a rigorous upper bound to the critical slope height or the factor of safety by assuming a reasonable slip surface. The application of kinematic theorem of limit analysis does not require the stresses field to be known, and results obtained have proved to be credible (Chen 1975). The limit analysis method has been widely used due to its efficiency and simplicity. Li *et al*. (2010) calculated the seismic displacement of slopes reinforced one row of piles, using the kinematic theorem of limit analysis within the framework of the pseudo-static approach. Zhao *et al*. (2016) carried out a comprehensive study on the seismic slope stability by considering cracks of any possible depth and location. Michalowski (2017) presented a new stability analysis for slopes with tensile strength cut-off in the framework of limit analysis. Xu *et al*. (2018) developed a series of stability charts, incorporating the influence of nonhomogeneity, anisotropy of soil and the pile reinforcement effects. Qin and Chian (2017) conducted a limit analysis on the kinematic stability of a two-stage slope in layered soils, with the upper part of the slope manmade. In their work, focuses were placed on the nonhomogeneity of the soil and the limit surcharge load. The effect of slope shape and depth coefficient was neglected. Moreover, the failure mechanism was limited. A more comprehensive study is yet to be carried out.

In this paper, the kinematic theorem of limit analysis is adopted to assess the seismic stability of a two-stage slope.

*Corresponding author, Professor
E-mail: raopingping@usst.edu.cn
[a]M.Sc. Student
E-mail: wujian6104@163.com
[b]Senior Engineer
E-mail: 2787806@qq.com
[c]Ph.D. Student
E-mail: 2475883143@qq.com
[d]Professor
E-mail: chqsh2006@163.com
[e]Professor
E-mail: Sanjay.Nimbalkar@uts.edu.au

ISSN: 2005-307X (Print), 2092-6219 (Online)

The seismic effect is taken into account by the pseudo-static approach. The failure mechanism is extended to include below-toe failure, toe failure and face failure. Based on the graphical method, the stability charts are presented to obtain the factor of safety without iteration. Parametric study involving the effect of slope geometry, internal friction angle, seismic effect as well as depth coefficient on the stability of a two-stage slope is carried out. Then the parametric effect on the critical failures is investigated.

2. Seismic stability analysis for a two-stage slope

2.1 Kinematic theorem of limit analysis

In the framework of limit analysis, the upper bound of true solution can be found by adopting the kinematic theorem which is a bifurcation of plasticity theory. The application of kinematic theorem requires that the rate of dissipation within the plastic zone be equated to the rate of external work of any assumed strain field which is governed by the normality rule and is compatible with the velocities at the boundary of the failing mass. The kinematic theorem of limit analysis method is elaborated and well employed in solving the slope stability problems by Chen (1975).

2.2 Work-energy balance equation and objective function

The prerequisite of kinematic theorem of limit analysis is that the soil is assumed to be perfectly plastic and the failure of soil mass satisfies the Mohr-Coulomb criterion as well as the associated flow rule. In this paper, the plane strain mechanism is considered, as shown in Fig.1. The two different slope angles of the slope are β_1 and β_2 respectively. The depth coefficient α is the ratio of upper height of the slope to the total slope height H. The region $ABCEF$, as a rigid block, rotates around the center of rotation O with the angular velocity ω. The failure surface of sliding soil mass is a rotational log-spiral discontinuity AF. The angle between the direct of velocity at each point on the discontinuity and failure surface equals to the internal friction angle φ. Other variables r_0, r_h, θ_h, θ_0, L and D defining the failure mechanism are indicated in Fig.1. The below-toe failure mechanism degenerates into the toe-failure mechanism as D=0. The expression of the log-spiral failure surface AF is:

$$r(\theta) = r_0 e^{(\theta-\theta_0)\tan\varphi} \tag{1}$$

The external work rate is composed of the rate of work due to soil weight and seismic force. The rate of work done by soil weight W can be calculated by subtracting the work done by region OAB, OBC, OCE and OEF from the work done by region OAB:

$$W_\gamma = \gamma\omega r_0^3 \left(f_1 - f_2 - f_3 - f_4 - f_5\right) \tag{2}$$

where γ is the unit weight of soil. The expressions of $f_1 \sim f_5$ are given as follows:

$$f_1 = \frac{1}{3\left(1+9\tan^2\varphi\right)}\left[\left(3\tan\varphi\cos\theta_h + \sin\theta_h\right)e^{3(\theta_h-\theta_0)\tan\varphi} - \left(3\tan\varphi\cos\theta_0 + \sin\theta_0\right)\right] \tag{3}$$

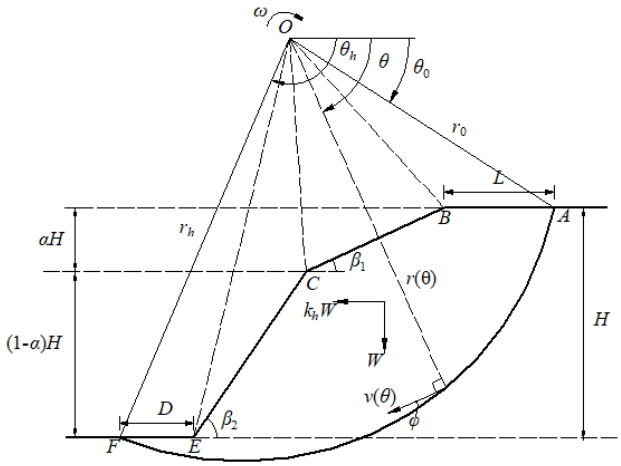

Fig. 1 Failure mechanism of a two-stage slope

$$f_2 = \frac{1}{6}\frac{L}{r_0}\sin\theta_0\left(2\cos\theta_0 - \frac{L}{r_0}\right) \tag{4}$$

$$f_3 = \frac{\alpha}{3}\frac{H}{r_0}\left(\cos\theta_0 - \frac{L}{r_0} + \sin\theta_0\cot\beta_1\right)\times\left(\cos\theta_0 - \frac{L}{r_0} - \frac{\alpha}{2}\frac{H}{r_0}\cot\beta_1\right) \tag{5}$$

$$f_4 = \frac{(1-\alpha)}{3}\frac{H}{r_0}\left[e^{(\theta_h-\theta_0)\tan\varphi}\left(\sin\theta_h\cot\beta_2 + \cos\theta_h\right) + \frac{D}{r_0}\right]\left[e^{(\theta_h-\theta_0)\tan\varphi}\cos\theta_h + \frac{D}{r_0} + \frac{(1-\alpha)}{2}\frac{H}{r_0}\cot\beta_2\right] \tag{6}$$

$$f_5 = \frac{1}{6}\frac{D}{r_0}\sin\theta_h\left[2\cos\theta_h e^{(\theta_h-\theta_0)\tan\varphi} + \frac{D}{r_0}\right]e^{(\theta_h-\theta_0)\tan\varphi} \tag{7}$$

Based on the geometric relations of slope, the following equations can be obtained:

$$\frac{L}{r_0} = \cos\theta_0 - \cos\theta_h e^{(\theta_h-\theta_0)\tan\varphi} - \frac{D}{r_0} - \frac{H}{r_0}\left[\alpha\cot\beta_1 + (1-\alpha)\cot\beta_2\right] \tag{8}$$

$$\frac{H}{r_0} = e^{(\theta_h-\theta_0)\tan\varphi}\sin\theta_h - \sin\theta_0 \tag{9}$$

Owing to the simplicity to be calculated, the pseudo-static approach is widely applied to the seismic analysis of stability for geotechnical structures. However, this approach ignores the seismic process (acceleration history) and does not discern the behavior of the structure. The effect of the seismic effect is represented by the force acting on the center of gravity. Herein, the vertical acceleration is ignored (Gazetas *et al.* 2009). The rate of work done by horizontal seismic force k_hW can be expressed as:

$$W_e = k_h\gamma\omega r_0^3\left(g_1 - g_2 - g_3 - g_4 - g_5\right) \tag{10}$$

where k_h is the horizontal seismic coefficient, and the expressions of $g_1 \sim g_5$ are given as follows:

$$g_1 = \frac{1}{3\left(1+9\tan^2\varphi\right)}\left[\left(3\tan\varphi\sin\theta_h - \cos\theta_h\right)e^{3(\theta_h-\theta_0)\tan\varphi} - \left(3\tan\varphi\sin\theta_0 - \cos\theta_0\right)\right] \tag{11}$$

$$g_2 = \frac{1}{3}\frac{L}{r_0}\sin^2\theta_0 \tag{12}$$

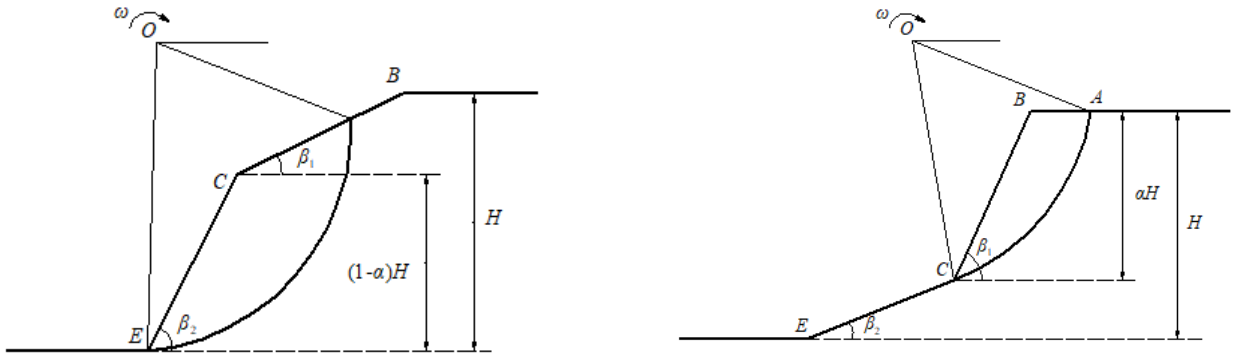

(a) Convex slope ($\beta_1<\beta_2$) (b) Concave slope ($\beta_1>\beta_2$)

Fig. 2 Face failure mechanism

$$g_3=\frac{\alpha}{3}\frac{H}{r_0}\left(\cos\theta_0-\frac{L}{r_0}+\sin\theta_0\cot\beta_1\right)\left(\sin\theta_0+\frac{\alpha}{2}\frac{H}{r_0}\right) \tag{13}$$

$$g_4=\frac{(1-\alpha)}{3}\frac{H}{r_0}\left[e^{(\theta_h-\theta_0)\tan\varphi}\left(\sin\theta_h\cot\beta_2+\cos\theta_h\right)+\frac{D}{r_0}\right]\left[e^{(\theta_h-\theta_0)\tan\varphi}\sin\theta_h-\frac{(1-\alpha)}{2}\frac{H}{r_0}\right] \tag{14}$$

$$g_5=\frac{1}{3}\frac{D}{r_0}\sin^2\theta_h e^{2(\theta_h-\theta_0)\tan\varphi} \tag{15}$$

The rate of internal dissipation D along failure surface AF can be expressed as:

$$D=\frac{c\omega r_0^2}{2\tan\varphi}\left[e^{2(\theta_h-\theta_0)\tan\varphi}-1\right] \tag{16}$$

where c is the cohesion of soil.

By equating the external work rate to the rate of internal dissipation, the dimensionless slope height can be obtained:

$$\frac{\gamma H}{c}=f\left(\theta_0,\theta_h,\frac{D}{r_0}\right) \tag{17}$$

where $f(\theta_0, \theta_h, D/r_0)$ is defined as:

$$f\left(\theta_0,\theta_h,\frac{D}{r_0}\right)=\frac{H}{r_0}\frac{1}{2\tan\varphi}\frac{e^{2(\theta_h-\theta_0)\tan\varphi}-1}{(f_1-f_2-f_3-f_4-f_5)+k_h(g_1-g_2-g_3-g_4-g_5)} \tag{18}$$

Then the stability factor N_S can be obtained:

$$N_S=\frac{\gamma H_c}{c}=\min f\left(\theta_0,\theta_h,D/r_0\right) \tag{19}$$

where H_c is the critical slope height.

The stability factor N_S is a function of three independent variables θ_0, θ_h and D/r_0. The minimum upper bound value of N_S can be found through the combination of Monte Carlo simulation and optimization algorithm with the following constraint conditions:

$$\begin{cases}0<\theta_0<\theta_h<\pi\\0<\alpha<1\\0\le D/r_0\end{cases} \tag{20}$$

3. Extended failure mechanism

Uilti (2013) proposed that the failure surface cannot go through the slope face for a single-stage slope under plane strain mechanism. Thereof, apart from toe failure and below-toe failure, the failure mechanism of a two-stage slope is extended to two types of face failures corresponding to the failure mechanism of a single-stage slope, as depicted in Fig. 2.

For a convex two-stage slope ($\beta_1<\beta_2$), the failure surface is supposed to pass through the slope toe E and the upper slope face BC. In consequence, this failure mechanism is regarded as toe failure of a single-stage slope with height $(1-\alpha)H$ and slope inclination β_2. The top surface CE of this single-stage slope is inclined at an angle β_1. The expressions of W_γ, W_e and D can be found in Gong *et al*. (2018). In the process of searching upper bound of stability factor, the slope height H should be replaced by $(1-\alpha)H$.

For a concave two-stage slope ($\beta_1>\beta_2$), the upper part of the two-stage slope could collapse while the rest remains stable. Consequently, the failure surface passes through the intersection of the slope face BC and CE. This failure mechanism is a special case of the mechanism presented in the paper when D=0 and $\beta_1=\beta_2$. However, the difference is that the slope height H should be replaced by αH during finding the best solution.

4. Comparison

To validate the effectiveness of the proposed method, the strength reduction method is herein employed to transform the stability factor to the factor of safety through iterative calculation for comparison, which is shown in Tables 1-3 for both single-stage slopes and two-stage slopes. As shown in Table 1, the factor of safety calculated in this paper is no larger than that in Gao *et al* (2013) which demonstrates the correctness of formula derivation and the superiority of solutions. Table 2 indicates that the differences among the results is no more than 9%, the largest of which appears in the static condition of $c/\gamma H$=0.17 and φ=17.5°. It is because the effect of vertical acceleration is ignored in current study that the factor of safety becomes larger than that of Graphical method and Iterative

Table 1 Comparation of factor of safety for a two-stage slope

Case	c /kPa	φ /°	γ /kN/m^3	α	β_1 /°	β_2 /°	H /m	Source	
								Gao *et al* (2013)	This paper
1	20	28	17.85	0.5	35	30	20	1.6028	1.5921
2	20	28	17.85	0.5	45	30	20	1.4676	1.4676

Table 2 Comparison of the factor of safety for a 45° slope (β_1=β_2)

$c/\gamma H$	φ /°	Source	k_h = 0	k_h = 0.1	k_h = 0.2
0.17	17.5	Graphical method*	1.663	1.401	1.192
		Iterative calculation*	1.652	1.394	1.201
		This paper	1.521	1.313	1.141
0.2	15	Graphical method*	1.748	1.474	1.256
		Iterative calculation*	1.754	1.472	1.262
		This paper	1.749	1.506	1.304
0.25	10	Graphical method*	1.877	1.551	1.321
		Iterative calculation*	1.878	1.561	1.323
		This paper	1.869	1.601	1.374

Note: *the factor of safety obtained from Qin and Chian (2018)

Table 3 Comparison of the factor of safety of two-stage slopes

k_h	Source	φ /°			
		15	20	25	30
0.0	Yang and Li (2018)	0.9333	1.1486	1.4495	1.8973
	This paper	0.9568	1.0809	1.2070	1.3369
0.1	Yang and Li (2018)	0.7664	0.9181	1.1162	1.3925
	This paper	0.8416	0.9506	1.0601	1.1733
0.2	Yang and Li (2018)	0.6436	0.7518	0.8957	1.0814
	This paper	0.7424	0.8385	0.9344	1.0330

calculation from Qin and Chian (2018) under seismic condition. The comparison of the factor of safety calculated from two different methods is shown in Table 3. Compared with force increase technique adopted by Yang and Li (2018), it can be seen that the largest difference can be nearly 30% under static condition with φ=30° for the reason that the effect of cohesion, internal friction angle and slope inclination on the calculation accuracy of force increase technique is higher than thatof strength reduction method. Hence, the proposed method to evaluate the stability of two-stage slopes is feasible.

5. Results and discussions

5.1 Stability charts

Based on the graphical method proposed by Qin and

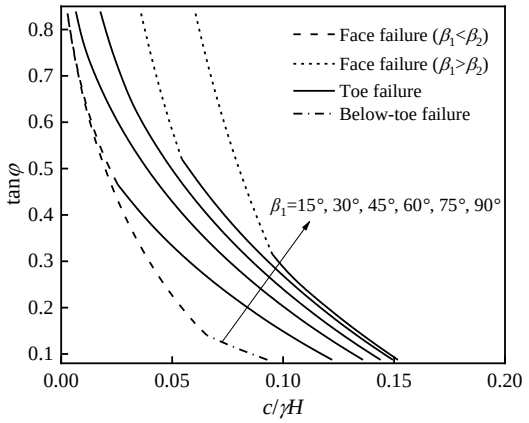

(a) β_2=45°

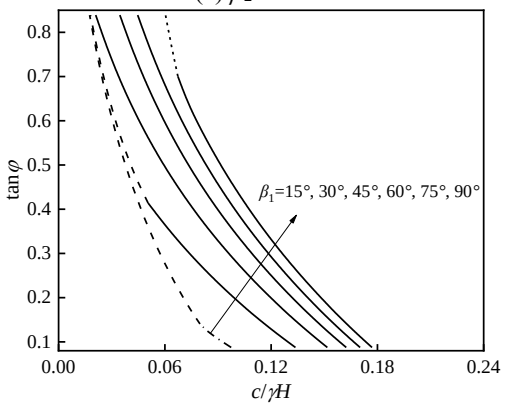

(b) β_2=60°

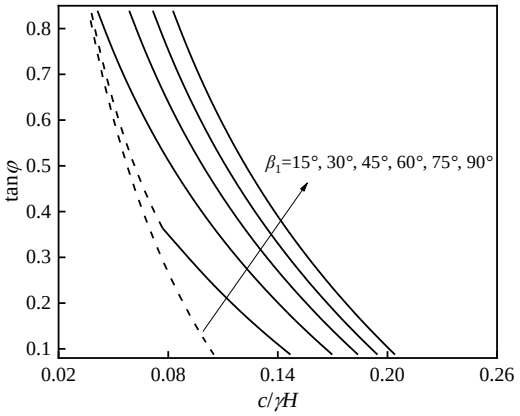

(c) β_2=75°

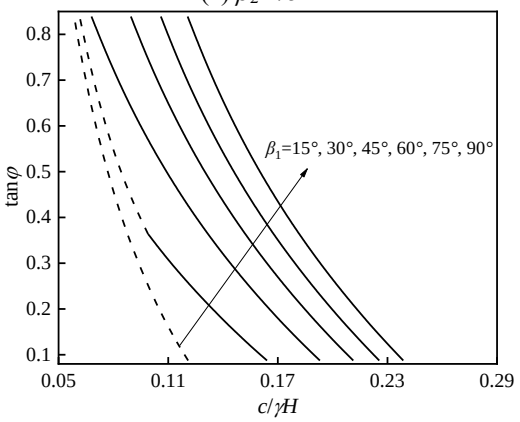

(d) β_2=90°

Fig. 3 Stability charts for a two-stage slope under static condition (k_h=0)

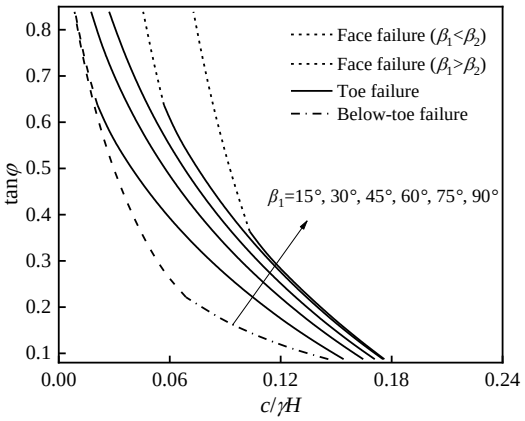

(a) β_2=45°

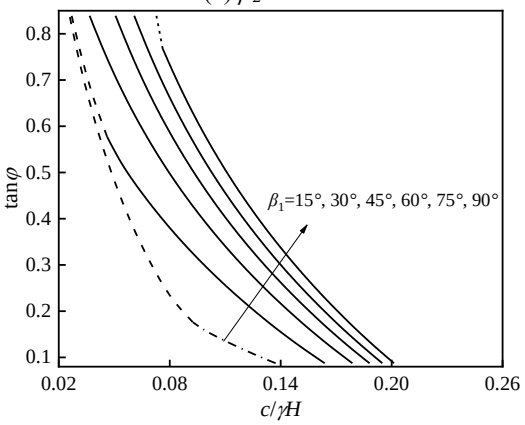

(b) β_2=60°

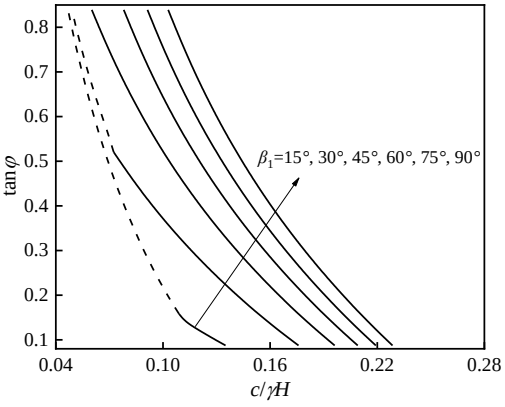

(c) β_2=75°

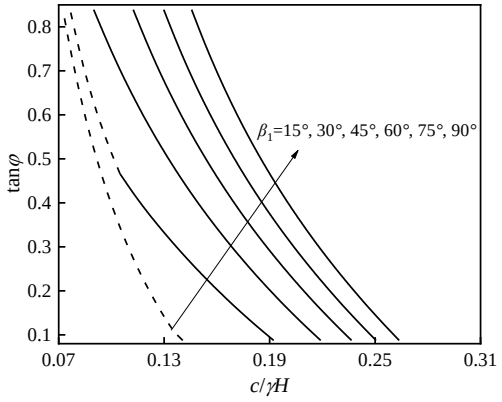

(d) β_2=90°

Fig. 4 Stability charts for a two-stage slope under seismic condition (k_h=0.1)

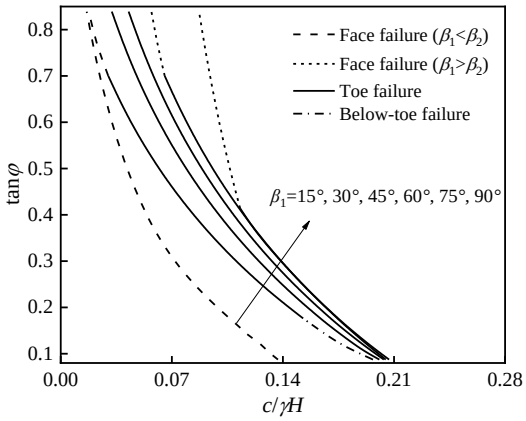

(a) β_2=45°

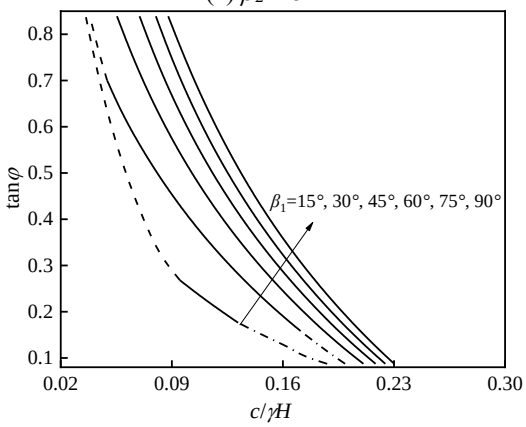

(b) β_2=60°

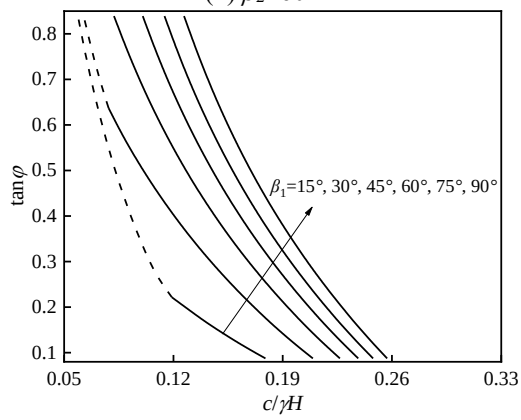

(c) β_2=75°

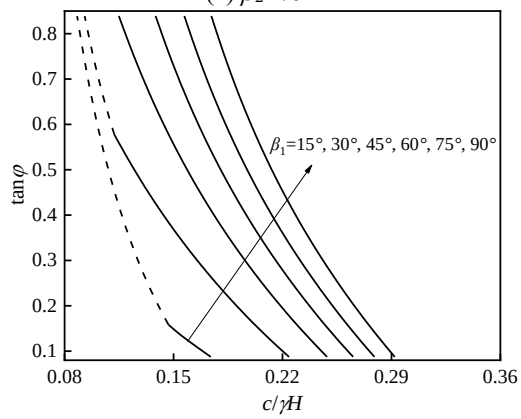

(d) β_2=90°

Fig. 5 Stability charts for a two-stage slope under seismic condition (k_h=0.2)

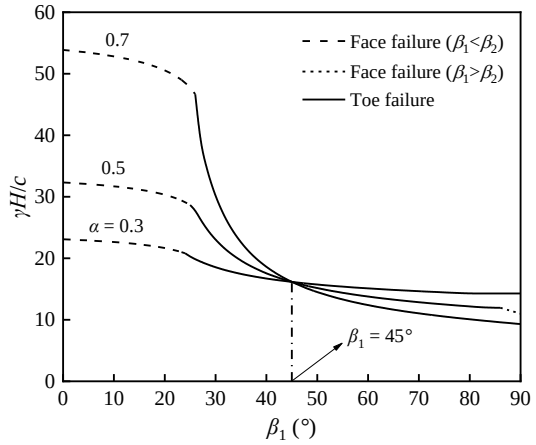

(a) k_h=0

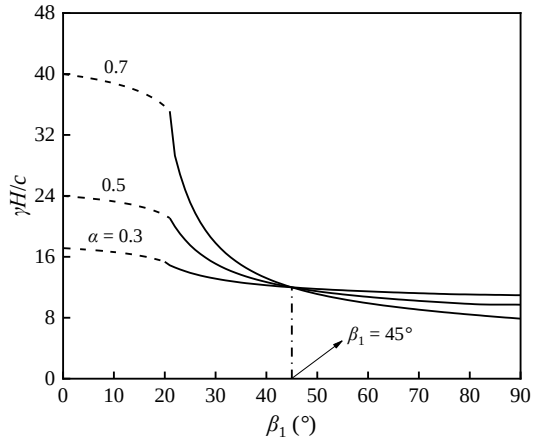

(b) k_h=0.1

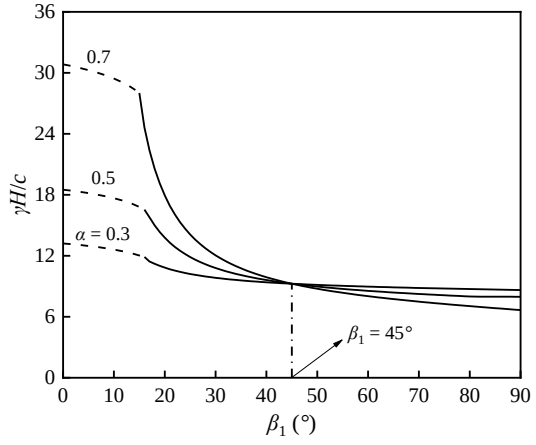

(c) k_h=0.2

Fig. 6 The effect of depth coefficient α on slope stability (β_2=45°, φ=20°)

Chian (2018), the factor of safety for a specific slope can be estimated conveniently without iteration from the correlations of $c/\gamma H$ and tanφ. Therefore, the stability charts are produced for a two-stage slope under both static and seismic condition, as illustrated in Figs. 3-5. It can be seen that the curve expands outward with an increase in β_1, indicating that the concave slope is susceptible to collapse. As expected, the presence of seismic effect makes the slope more unstable. Explicitly, failure mechanism is illustrated in

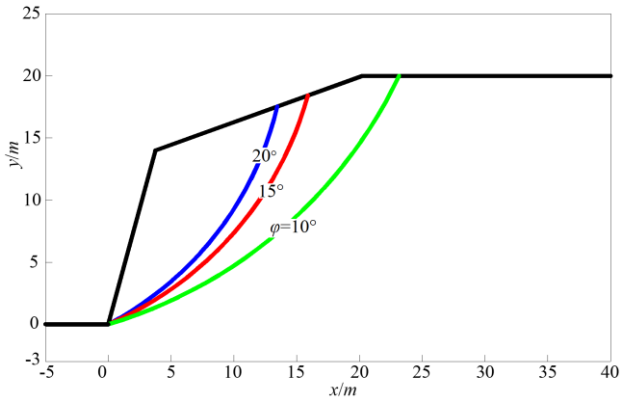

(a) β_1=20°, β_2=75°

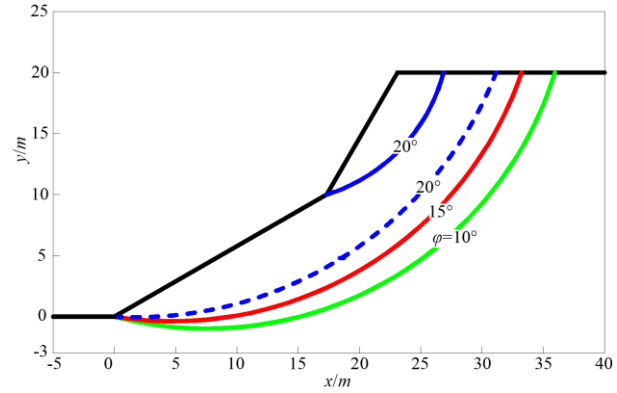

(b) β_1=60°, β_2=30°

Fig. 7 Critical failure surfaces with different internal friction angle under static condition

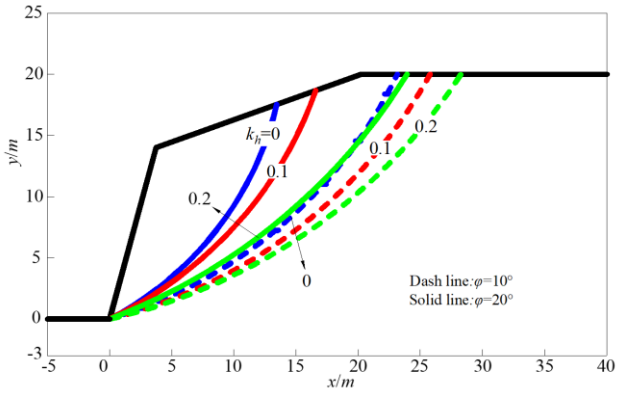

(a) β_1=20°, β_2=75°

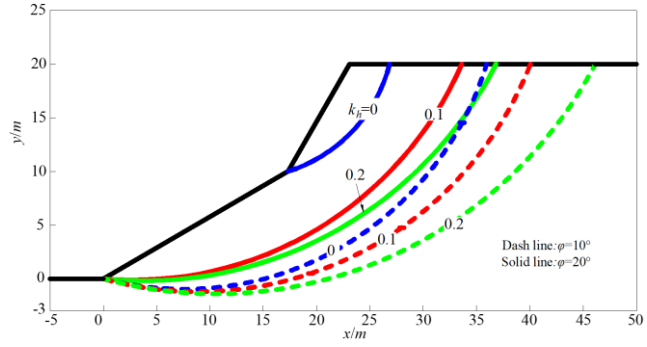

(b) β_1=60°, β_2=30°

Fig. 8 Critical failure surfaces with different horizontal seismic coefficient k_h

stability charts. It is toe failure that is the critical failure mechanism in most cases. A convex slope with lower β_1 and β_2 is more likely to induce face failure. Although the face failure occurs to a concave slope with larger β_1 and lower β_2 as well, the curve of $c/\gamma H$ and $\tan\varphi$ of a concave slope is on the outside of that of a convex slope, which means a convex slope is more stable than a concave slope. Only with lower $\tan\varphi$ is the below-toe failure induced for a two-stage slope. Simultaneously, the mutation of curve occurs between the transition of failure mechanism. Moreover, the presence of seismic effect amplifies the possibility of below-toe failure and reduces the possibility of face failure. Take two examples. For $\tan\varphi$=0.15, a convex slope with β_1=30° and β_2=45° undergoes toe failure under static condition, but below-toe failure under k_h=0.2; for $\tan\varphi$=0.35, a concave slope with β_1=90° and β_2=45° undergoes face failure under static condition, but toe failure under k_h=0.2;

Fig. 6 presents the effect of depth coefficient α on two-stage slope stability. Without exception, α has no influence on the slope stability when a two-stage slope degrades to a sing-stage slope. Furthermore, Fig .6 shows that there is a turning point about the effect of α on the slope stability where a two-stage slope transfers from a convex slope to a concave slope. For a convex slope, N_S increases considerably with the increase in α because the two-stage slope becomes gentler as α increases. Conversely, the opposite tendency can be observed for a concave slope. Similarly, the cause lies in the fact that the increase in α is equivalent to the increase in the inclination of a concave slope. Note that the failure mechanism of a convex slope is transformed from face failure to toe failure as an increase in β_1 and strong seismic excitation reduces the possibility of occurrence of face failure, indicating a larger scale of slope collapse.

5.2 Parametric effect on the critical failure surface

The effect of internal friction angle φ on the critical failure surface is illustrated in Fig. 7. The critical failure surface is sensitive to φ. A deeper failure surface is likely to occur with the decrease in φ. As is depicted in Fig. 7(b), the stability factor N_S calculated with φ=20° based on the toe-failure mechanism (dash line) and the face-failure mechanism (solid line) are 21.63 and 20.78 respectively, which implies that only the consideration of toe failure and below-toe failure for a two-stage slope leads to a conservative assessment to slope stability. The effect of horizontal seismic coefficient k_h on the critical failure surface is presented in Fig. 8. It can be seen that an increase in k_h leads to a deeper failure surface. For the specific parameters, the critical failure mechanism transfers from face failure to toe failure as k_h increases, presenting the severity of slope collapse.

6. Conclusions

The coupled kinematic theorem of limit analysis with the pseudo-static method is adopted to assess the seismic stability of a two-stage slope. The failure mechanism is extended to include below toe failure, toe failure and face failure. Parametric studies are carried out and the main conclusions are given as follows:

The geometry of a two-stage slope has dramatical influences on two-stage slope failure mechanism. In comparison with the single-stage slope, the convex two-stage slope has a higher capacity to sustain seismic excitation, while the concave two-stage slope has a lower capacity. The toe failure is determined as the critical failure mechanism in most cases. For a concave slope with lower β_2, the upper part of the two-stage slope could lose stability, indicating that face failure is more critical. The slope could become more stable with the increase in depth coefficient α for a convex slope. On the contrary, larger α is detrimental for a concave slope. A deeper failure surface can be obtained by decreasing internal friction angle φ or increasing horizontal seismic coefficient k_h.

Acknowledgments

This work is supported by the National Natural Science Foundation of China (Project No.: 42077435). The authors wish to express their gratitude for the above financial support.

References

Aksoy C.O., Uyar, G.G. and Ozcelik, Y. (2016), "Comparison of Hoek-Brown and Mohr-Coulomb failure criterion for deep open coal mine slope stability", *Struct. Eng. Mech.*, **60**(5), 809-828. https://doi.org/10.12989/sem.2016.60.5.809.

Babanouri, N. and Sarfarazi, V. (2018), "Numerical analysis of a complex slope instability: pseudo-wedge failures", *Geomech. Eng.*, **15**(1), 669-676. http://doi.org/10.12989/gae.2018.15.1.669.

Chen, W.F. (1975), *Limit Analysis and Soil Plasticity*, Elsevier Scientific Publishing Company, New York, U.S.A.

Cai, F. and Ugai, K. (2000), "Numerical analysis of the stability of a slope reinforced with piles", *Soils Found.*, **40**(1), 73-84. https://doi.org/10.3208/sandf.40.73.

Deng, D.P., Li, L. and Zhao, L.H. (2017), "Limit-equilibrium method for reinforced slope stability and optimum design of antislide micropile parameters", *Int. J. Geomech.*, **17**(2), 06016019. http://doi.org/10.1061/(ASCE)GM.1943-5622.0000722.

Gazetas G., Garini E., Anastasopoulos I. and Georgarakos T. (2009), "Effects of near-fault ground shaking on sliding systems", *J. Geotech. Geoenviron. Eng.*, **135**(12), 1906-1921. https://doi.org/10.1061/(ASCE)GT.1943-5606.0000174.

Gao L. S., Zhao L.H., Tang G.P. and Luo W. (2013), "Upper bound limit analysis of stability on inhomogeneity and anisotropy two-stage slope", *Electron. J. Geotech. Eng.*, **18**, 3581-3604.

Gong, W.B., Li, J.P. and Li, L. (2018), "Limit analysis on seismic stability of anisotropic and nonhomogeneous slopes with anti-slide piles", *Sci. China Technol. Sc.*, **61**(1), 140-146. https://doi.org/10.1007/s11431-017-9147-8.

Kim, Y.M. and Jeong, S.S. (2017), "Modelling of shallow landslides in an unsaturated soil slope using a coupled model", *Geomech. Eng.*, **13**(2), 353-370. https://doi.org/10.12989/gae.2017.13.2.353.

Lam, L. and Fredlund, D.G. (1993), "A general limit equilibrium

model for three-dimensional slope stability analysis", *Can. Geotech. J.*, **30**(6), 905-919. https://doi.org/10.1139/t93-089.
Li, X.P., He, S.M. and Wu, Y. (2010), "Seismic displacement of slopes reinforced with piles", *J. Geotech. Geoenviron.*, **136**(6), 880-884. https://doi.org/10.1061/(asce)gt.1943-5606.0000296.
Michalowski, R.L. (2017), "Stability of intact slopes with tensile strength cut-off", *Geotechnique*, **67**(8), 720-727. https://doi.org/10.1680/jgeot.16.P.037.
Motlagh, A.T., Ghanbari, A., Maedeh, P.A. and Wu, W. (2018), "A new analytical approach to estimate the seismic tensile force of geosynthetic reinforcement respect to the uniform surcharge of slopes", *Earthq. Struct.*, **15**(6), 687-699. https://doi.org/10.12989/eas.2018.15.6.687
Qin, C.B. and Chian, S.C. (2017), "Kinematic stability of a two-stage slope in layered soils", *Int. J. Geomech.*, **17**(9), 06017006. https://doi.org/10.1061/(ASCE)GM.1943-5622.0000928.
Qin, C.B. and Chian, S.C. (2018), "New perspective on seismic slope stability analysis", *Int. J. Geomech.*, **18**(7), 06018013. https://doi.org/10.1061/(ASCE)GM.1943-5622.0001170.
Shukla, S.K., Khandelwal, S., Verma, V.N. and Sivakugan, N. (2009), "Effect of surcharge on the stability of anchored rock slope with water filled tension crack under seismic loading condition", *Geotech. Geol. Eng.*, **27**(4), 529-538. https://doi.org/10.1007/s10706-009-9254-3.
Shen, H. and Abbas, S.M. (2013), "Rock slope reliability analysis based on distinct element method and random set theory", *Int. J. Rock Mech. Min. Sci.*, **61**(10), 15-22. https://doi.org/
Tran, T.P., Kim, A.R. and Cho, G.C. (2019), "Numerical modeling on the stability of slope with foundation during rainfall", *Geomech. Eng.*, **17**(1), 109-118. https://doi.org/10.12989/gae.2019.17.1.109.
Utili S. (2013), "Investigation by limit analysis on the stability of slopes with cracks", *Geotechnique*, **63**(2), 140-154. https://doi.org/10.1680/geot.11.p.068.
Xu, J.S., Li, Y.X. and Yang, X.L. (2018), "Stability charts and reinforcement with piles in 3D nonhomogeneous and anisotropic soil slope", *Geomech. Eng.*, **14**(1), 71-81. https://doi.org/10.12989/gae.2018.14.1.071.
Yang, M., Su, H.Z. and Wen, Z.P. (2017), "An approach of evaluation and mechanism study on the high and steep rock slope in water conservancy project", *Comput. Concrete*, **19**(5), 527-535. https://doi.org/10.12989/cac.2017.19.5.527.
Yang, X.L. and Li, Z.W. (2018), "Factor of safety of three-dimensional stepped slopes", *Int. J. Geomech.*, **18**(6), 04018036. https://doi.org/10.1061/(ASCE)GM.1943-5622.0001154.
Zhao, L.H., Cheng, X., Zhang, Y.B., Li, L. and Li, D.J. (2016), "Stability analysis of seismic slopes with cracks", *Comput. Geotech.*, **77**, 77-90. https://doi.org/10.1016/j.compg eo.2016.04.007.

GC